Practical Realization of an Improved Photovoltaic Grid Integration with MPPT

Neeraj Priyadarshi*‡, Amarjeet Kumar Sharma*, S Priyam*

*Department of Electrical Engineering, MIT Purnea-854301, INDIA

‡ Corresponding Author; Neeraj Priyadarshi, neerajrjd@gmail.com

Received: 10.04.2017 Accepted:13.05.2017

Abstract- To maximize the photovoltaic (PV) tracking efficiency, maximum power point trackers (MPPT) are essential components. Here a 200 W grid connected PV power system is considered for efficient realization. The fuzzy logic controller (FLC) controlled MPPT method has been employed to obtain the optimal power from PV module. Also, a zeta buck –boost converter is proposed to reduce ripple in output which work as a MPPT tracker and provide amplification and reduction in input voltage level without polarity inversion. Space vector pulse width modulation (SVPWM) based 3- phase voltage source inverter (VSI) is employed as it has better dc link utilization, fast dynamic response, low switching losses and fixed switching pattern compared to other conventional current control. The simulation model is designed using MATLAB/Simulink environment and validated through real time dSPACE experimental control. The tracking and inverter efficiency of the grid PV system have been obtained practically at different sun insolation level.

Keywords: FLC, MPPT, MATLAB, PV, SVPWM, VSI.

1. Introduction

Conventionally fossil fuels are used for generation of electrical power. But harmful gases are produced after burning of these fuels. In case of nuclear fission, radioactive wastes are generated due to material long time dead. Renewable energies become a promising source of energy and it plays an important role to provide alternative power generation [1-6]. Because of green, enormous availability and environmental friendliness nature it is used in many applications which is growing exponentially worldwide. Now a days, grid connected photovoltaic system is installed to obtain alternate source of energy. However, the present photovoltaic (PV) system has very less conversion efficiency. As photovoltaic system depends on variable irradiance and ambient temperature, so it must be supplemented by the additional technology to supply the demand characteristics. The maximum power point tracking (MPPT) trackers are the additional technology provided to obtain PV peak power. Various MPPT techniques have been studied in literature [7-9]. The classical MPPT methods are fail to track optimum power from PV module under variable weather conditions. Here a modified fuzzy logic controller (FLC) based intelligent MPPT control is considered. Compared to conventional MPPT algorithm, the FLC based MPPT has high convergence speed, better precise response and high tracking efficiency. Several dc-dc converters have been implemented for employment of maximum output from PV module such as cuk converter, sepic converter, four switch types, zeta converter [10-12]. Among all dc-dc converters zeta converters have better tracking power capability as well as low ripple content in output [13]. Moreover, there are numerous inverter control methods of 3 phase inverter have been discussed [14-15]. Among all inverter control methods, the space vector pulse width modulation (SVPWM) using dSPACE controller interface is proposed in this research work [16]. It has better dc link utilization, fast dynamic response, low switching losses and fixed switching pattern compared to other conventional current control. Nambiar et al [17] discussed only simulation implementation of fuzzy logic based grid connected wind energy system using boost converter. Moreover, the performance of inverter current control for grid connected wind energy system is also evaluated. However, in this study the author's have used triangular membership function. The performance of the MPPT controller is not suitable under adverse weather conditions. Morever, the inverter controlled by current control is not able to inject sinusoidal current to the utility grid. Therefore, In this research work for improvement of tracking and inverter efficiency, the zeta converter controlled FLC based MPPT with SVPWM current control for PV grid connected system has been implemented experimentally. The simulation and experimental responses verify the effectiveness of grid integrated PV system using dSPACE control board. In this research work the novelty of proposed zeta converter is generation of gating pulses using dSPACE real time control board with FLC controller. The experimental tracking and inverter efficiency have also been presented under different sun insolation.

2. Structure of Grid Integrated PV System with MPPT

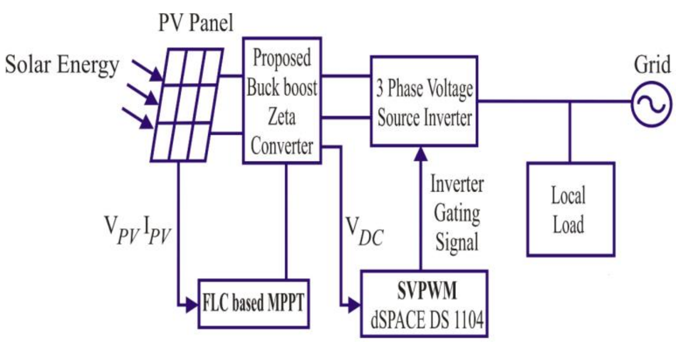

Fig. 1 Block diagram of proposed Grid integration

The proposed system depicted in Fig 1 comprises of a PV array, proposed zeta buck boost converter 3- phase voltage source inverter (VSI) grid integration. The proposed zeta buck boost converter and 3-phase VSI is controlled by fuzzy logic controller and SVPWM method, respectively. The voltage and current from the PV panel is sourced by FLC. The MPPT is performed through zeta buck boost converter, which extracts optimal power from the PV panel. The DC output from the zeta converter is converted into AC power using inverter and it is injected into utility grid. The output DC voltages from the zeta buck boost converter feedback as an input to the SVPWM controller.

2.1 Mathematical modeling of PV Cell

On the basis of equivalent PV cell circuit shown in Fig 2, the mathematical relations are based on the environmental factors as temperature and solar insolation. The PV cell model has been constructed.

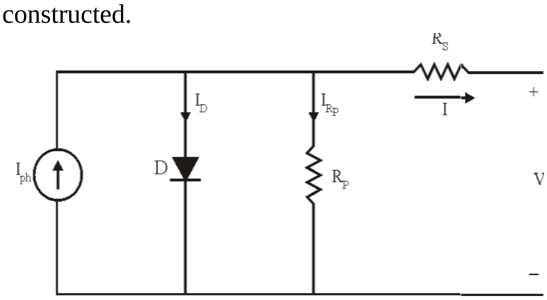

Fig. 2 PV cell basic current

From above PV cell circuit , we can write:

$$I = I_{Ph} - I_D - I_{R_p} \quad (1)$$

$$I_D = I_o * \exp\left[\left(\frac{qv}{AK\,T_C}\right) - 1\right] \quad (2)$$

$$I_0 = I_{or}\left[\frac{T_c}{T_r}\right]^3 \exp\left[\frac{q\,Eq}{AK}\left(\frac{1}{T_r} - \frac{1}{T_c}\right)\right] \quad (3)$$

Where,

I_{ph}	=	Photon current,
I_0	=	Current in reverse saturation,
q	=	Charge on electron,
V	=	Cell output voltage,
K	=	Boltzmann's constant,
T_c	=	Cell operating temperature,
A	=	Diode ideality factor,
Rs	=	Cell Series resistor
R_P	=	Cell shunt resistor
I_{or}	=	Reverse saturation current at temperature T_r.
E_q	=	Semi conductor band gap energy (J)
I_D	=	Diode current
I_{RP}	=	Current through parallel resistor
Tr	=	Temperature at standard test conditions

The PV specifications like open circuit voltage (V_{oc}), short circuit current (I_{sc}), peak power (V_m) and peak current (I_m) decided by industry is matched with parameters of ideal PV module.

Here $I_{Ph} = I_{sc}$ since $R_s < 1\Omega$ and in case of open circuit state, I = 0, V = V_{oc}

$$I = I_{sc}\left\{1 - K_1\left[\exp\left(\frac{V}{K_2 * V_{OC}}\right)\right] - 1\right\} \quad \textbf{(4)}$$

Under maximum power point state when V = V_m, I =I_m

$$I_m = I_{SC}\left\{1 - K_1\left[\exp\left(\frac{V_m}{K_2 * V_{OC}}\right)\right] - 1\right\} \quad \textbf{(5)}$$

At Normal temperature,

$$\exp\left(\frac{V_m}{K_2\,V_{OC}}\right) >> 1, \quad K_1 = \left(1 - \frac{I_m}{I_{SC}}\right)\exp\left(\frac{-V_m}{K_2\,V_{OC}}\right) \quad (6)$$

In case of open circuit state, when I = 0, V = V_{OC}

$$0 = I_{SC}\left\{1 - \left(1 - \frac{I_m}{I_{SC}}\right)\exp\left(\frac{-V_m}{K_2\,V_{OC}}\right)\left[\exp\left(\frac{1}{K_2}\right) - 1\right] - 1\right\} \quad (7)$$

At Normal temperature

$$\exp\left(\frac{1}{K_2}\right) >> 1, \quad K_2 = \left(\frac{V_m}{V_{OC}} - 1\right)\Big/ \ln\left(1 - \frac{I_m}{I_{SC}}\right) \quad (8)$$

For PV cell modeling the parameters V_{oc}, I_{sc}, V_m, I_m, K_1 and K_2 can be calculated.

Considering variable environmental temperature and solar irradiance, the model can be expressed as [18]:

$$T_c = T_a + t_c S \tag{9}$$

$$I = I_{SC}\left\{1 - K_1\left[\exp\left(\frac{V - dV}{K_2 V_{OC}}\right) - 1\right]\right\} + dI \tag{10}$$

Where

$$dI = \alpha \cdot \frac{S}{S_{ref}} \cdot dT + \left(\frac{S}{S_{ref}} - 1\right) \cdot I_{SC} \tag{11}$$

Eqn 12 and 13 denotes the small change in PV voltage (dV) and operating cell temperature (dT) as:

$$dV = -\beta dT - Rs.dI \tag{12}$$

$$dT = T_C - Tref \tag{13}$$

Where,

S = Operating Sun insolation

S_{ref} = Reference solar radiation

R_s = Series internal resistance

T_{ref} = Reference temperature

β = Open circuit voltage temperature coefficient

α = Short circuit current temperature coefficient.

t_c = Initial cell operating temperature

T_C = Cell operating temperature

T_a = Ambient Temperature

Based on the mathematical modeling of PV systems, the 200 W PV systems have been designed in MATLAB/Simulink environment shown in Fig 3. Table 1 shows the electrical specification of 200 W PV systems.

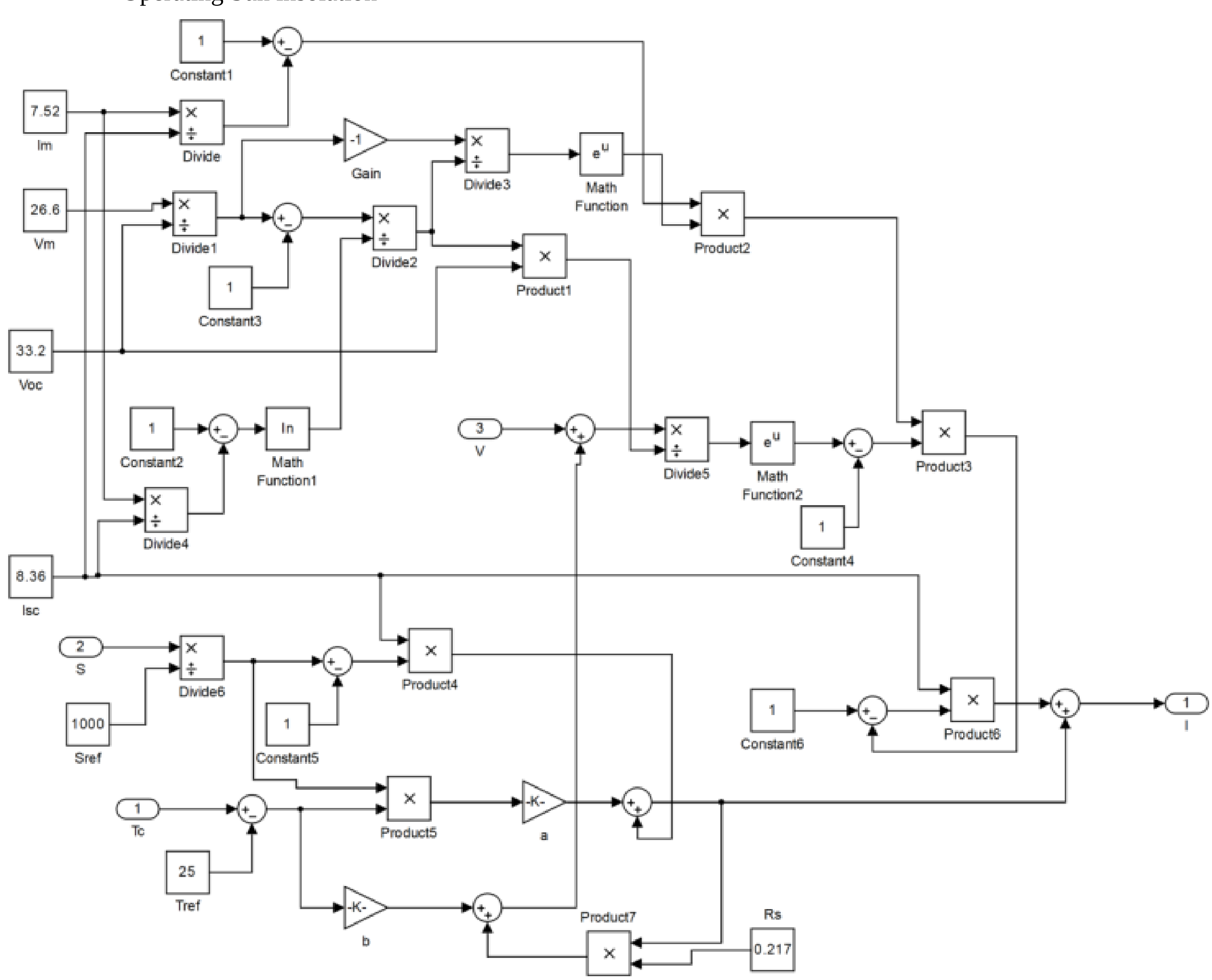

Fig. 3 MATLAB/Simulink implementation of 200 W PV system

MATLAB simulated I-V and P-V curves are presented in Fig. 4, with varying irradiance level and at constant ambient temperature of 25 ^{0}C. Also, Fig. 5 presents the simulated I-V and P-V responses, when external temperature is varying and irradiance level is maintained constant at 1000 W/m^2. The simulation has been performed under standard test conditions (STC) (S = 1000 W/m^2 and T = 25 ^{0}C).

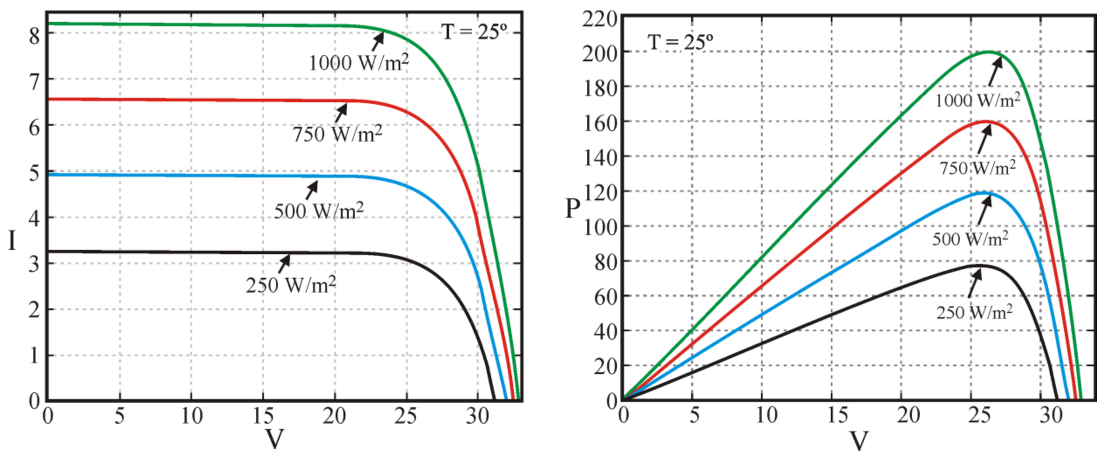

(a) (b)

Fig .4: Responses of PV array at varying irradiance and constant ambient temperature using MATLAB/Simulink
(a) I-V Characteristics (b) P-V Characteristics

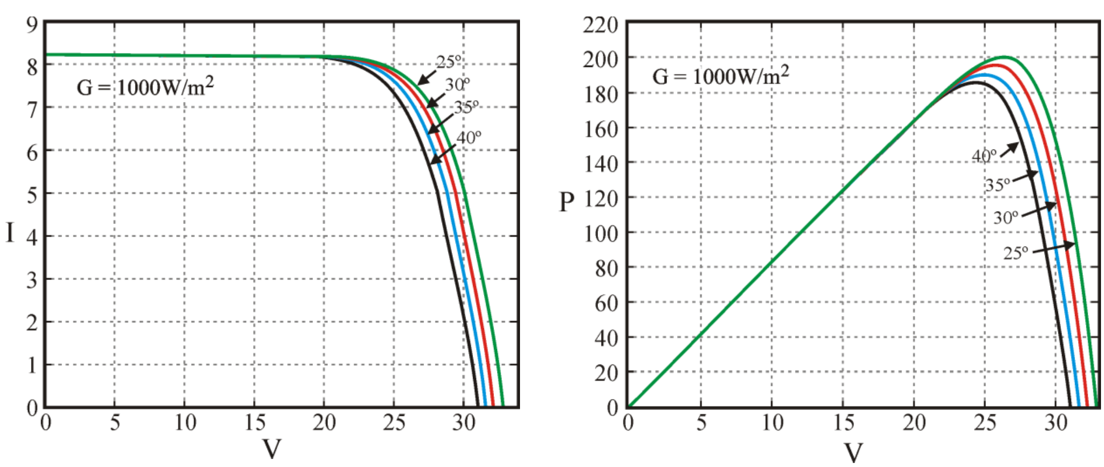

(a) (b)

Fig. 5: Responses of PV array at constant irradiance and variable ambient temperature using MATLAB/Simulink
(a) I-V Characteristics (b) P-V Characteristics

2.2 Mathematical Modeling of Proposed Zeta Converter

In this research work, zeta converter has been employed as a MPPT tracker. Because of two inductors and capacitors it steps up and down the supply voltage without polarity change. Also, the proposed converter works in two modes of operation as switch is opened and closed. The inductors L and L_1 through current flows and diode is reverse biased during switch closed condition. The L_1 inductor transferred the energy to R_L and diode conducts in case of opened switch condition as shown in Fig 6. Table 2 presents the specifications of zeta buck-boost converter used for simulation as well as experimentation.

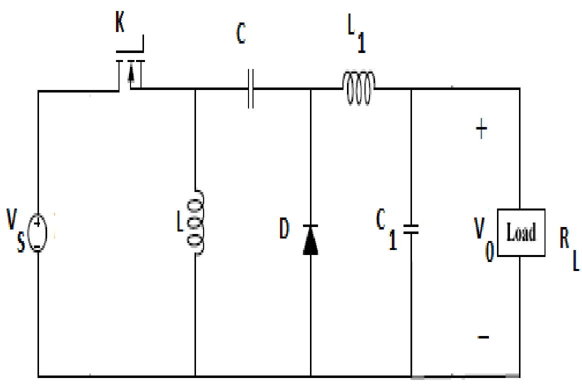

Fig. 6 Circuit of zeta converter

Table 1: Electrical Specifications of 200 W PV panel

PV Panel Parameters	**Value**
Maximum Power	200 W
Max. Voltage	26.6 V
Max. Current	7.52 A
V_{oc}	33.2 V
I_{sc}	8.36 A
Temperature coefficient of I_{SC} (K_i) = 5.02* 10^{-3} A/ ^{0}C	5.02* 10^{-3} A/ ^{0}C
Temperature coefficient of V_{OC} (K_V)	-1.20*10^{-1} V/ ^{0}C

Apply KVL in the zeta buck boost converter circuit, the ripple inductor currents and ripple capacitor voltages can be expressed as:

$$\Delta I_1 = \frac{DV_S}{f_s L} \quad (14)$$

$$\Delta I_2 = \frac{DV_S}{f_s L_1} \quad (15)$$

$$\Delta V_C = \frac{DV_S}{8CLf_s^2} \quad (16)$$

$$\Delta V_{C_1} = \frac{DV_S}{8C_1 L_1 f_s^2} \quad (17)$$

The zeta converter's inductor and capacitor critical values are written as:

$$L \geq R_L * (1-D)^2 / 2Df_s \quad (18)$$

$$L_1 \geq \frac{(1-D)\ R_L}{2 f_s} \quad (19)$$

$$C \geq \frac{D}{8(1-D) f_s R_L} \quad (20)$$

$$C_1 \geq \frac{1}{D f_s R_L} \quad (21)$$

Where D=Duty ratio and f_s=Switching frequency

Table 2: PARAMETERS OF ZETA BUCK-BOOST CONVERTER

Parameters	**Values**
Capacitor(C,C_1)	3.45e-4F
Inductance(L,L_1)	23.8mH
Resistance	30Ω
Switching Frequency	20KHz

2.3 Proposed Fuzzy Logic based MPPT controller

In this paper FLC based MPPT algorithm has been proposed to improve the tracking power of PV array which does not require mathematical modeling and able to handle non-linear operating conditions. Because of variable irradiance level the conventional MPPT methods produces low tracking efficiency with high power oscillation around maximum power point (MPP). Here FLC based MPPT is considered as it gives fast dynamic response, high tracked efficiency, with better convergence speed compared to classical MPPT algorithms. Under changing environmental conditions, the proposed FLC MPPT achieves optimal power from PV modules. The fuzzification, defuzzification and rule base are the main components comprised by FLC controller depicted in Fig 7. where error E (input1) and change in error dE (input2) are the two inputs.

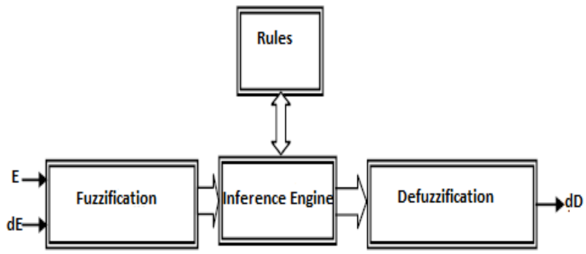

Fig. 7 Structure of FLC

Fuzzification:

Fuzzification is the method to convert crisp value to Fuzzy value. Inputs to the fuzzification block, error E (input1) and change in error dE (input2), dE can be obtained by following relation.

$$E = P_{PV(s)} - P_{PV(s-1)} / I_{PV(s)} - I_{PV(s-1)} \quad (22)$$

$$dE = E(s) - E(s-1) \quad (23)$$

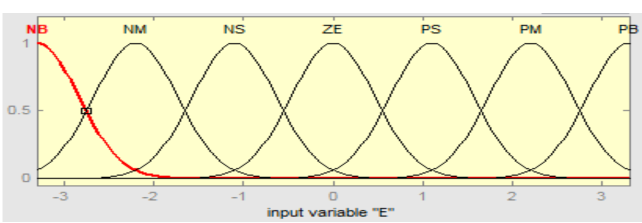

(a)

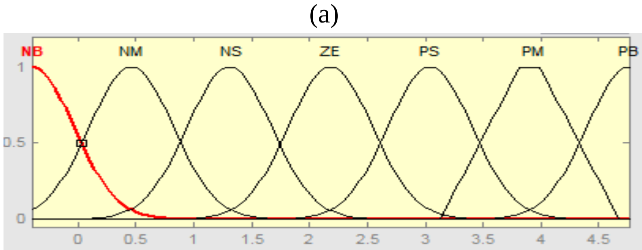

(b)

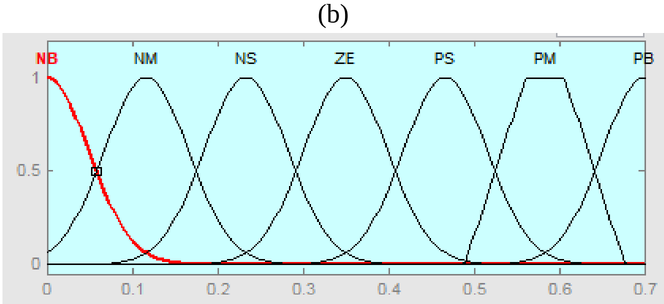

Fig.8 (a) Membership function E (b) Membership function dE (c) Membership function Output D

Where Ppv(s) and Ipv(s) are the power and current of PV array, respectively. E and dE acts as an input to the fuzzification which generates optimal duty ratio for power switch of zeta converter. The ΔP(s)/ΔI(s) obtained using (22) & (23). The input and output variables are assigned with 7 linguistic variables as shown in Fig 8(a), (b) and (c).

Table 3: Fuzzy inference rules

dE*E	NB	NM	NS	ZE	PS	PM	PB
NB	PM	NB	PM	PS	ZE	PS	ZE
NM	PS	PS	NB	NB	PB	PM	PS
NS	NM	PM	ZE	NM	NB	ZE	PM
ZE	ZE	NM	NS	PM	NS	NB	NM
PS	PB	ZE	NM	ZE	NM	NS	NB
PM	NB	NB	PB	PB	PM	PS	ZE
PB	PS	NS	PS	ZE	PB	NM	PS

Fuzzy *Inference engine (Fuzzy rule base):* The Mamdani's max-min composition method is employed to make fuzzy decision. 49 fuzzy rules have been created and presented in Table 3.

Defuzzification:

Defuzzification method is used to get numerical variable of the output of FLC. It converts linguistic variable to physical variable. Defuzzification is based on centroid method which achieves optimal duty ratio to the zeta converter as a reference signal. The optimum value of Duty cycle is to be sent to the MOSFET of zeta buck-boost converter as a reference signal.

3. PV Inverter Controller

The program interface using library block set is carried out using dSPACE control algorithm. Prototype has been implemented using real time simulation interface.

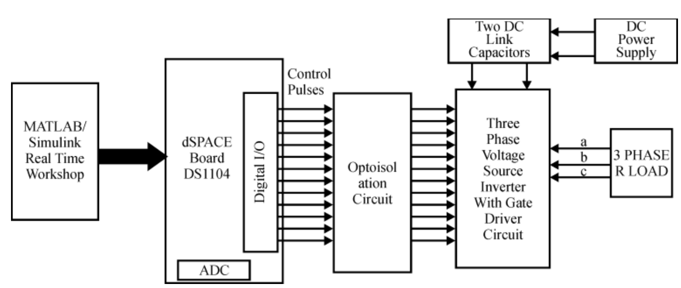

Fig. 9 VSI inverter control using dSPACE DS1104 control board

The switching pulses for 3-phase inverter are generated using interface of MATLAB/Simulink and dSPACE digital processor. The space vector pulse width modulation (SVPWM) is performed using dSPACE DS 1104 real time board. The major components employed for its control is presented by Fig 9. For isolation of DSP master bit I/O in RTI Library block an opto-isolated interface circuit is used. MPC8240 of 64 bit with PPC603e core processor is used to perform the interface of MATLAB/Simulink with dSPACE DS1104. The MATLAB/Simulink simulated model is converted and compiled to C language which automatically interfaces to the dSPACE board. For this purpose DS1104ADC, DS1104BIT OUT and DS1104DAC input/output interfacers have been used. Moreover, the complete performance analysis of 3-phase inverter is analyzed through graphical user interface of control desk. The dSPACE, voltage and current sources are employed as major components for hardware design which is presented by Fig 10. The output from inverter is integrated to utility grid through point of common coupling (PCC).

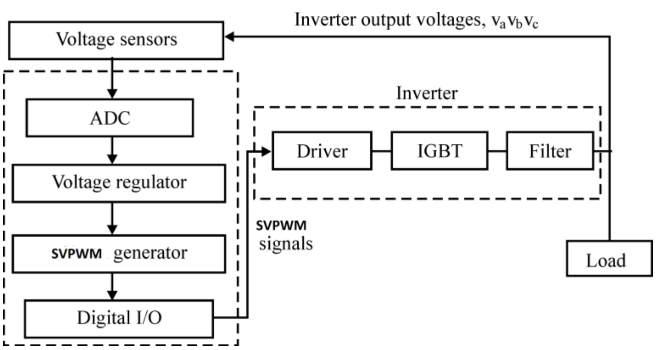

Fig. 10 Structure of inverter dSPACE control.

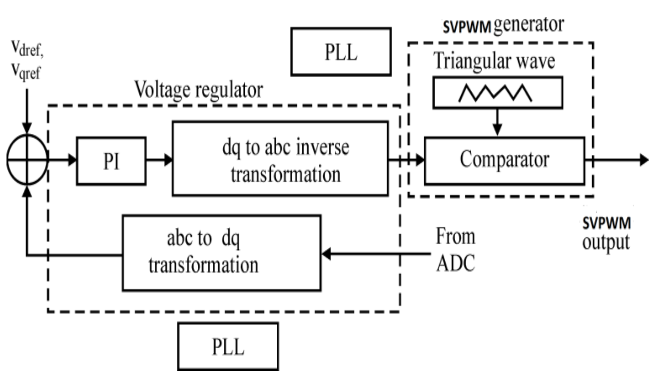

Fig. 11 Closed loop voltage control of dSPACE board

3- Phase voltage measurement sensors are employed for the interface purpose of inverter output voltage which attenuates the output of inverter with supplement gain to achieve the dSPACE adaptation voltage. After scaling down it through A/D converter to the dSPACE board, the ADC voltage is regulated using voltage regulator. The abc-dq transformation is done by application of Park's transformation. v_d and v_q components are regulated on their respective references v_{dref} and v_{qref} respectively which is depicted in Fig 11. The 50 Hz synchronized signal from PLL has been obtained for balance load operating condition.

4. Simulation Results

To validate the effective characteristics of proposed controller design, the MATLAB/Simulink environment is employed. Under standard irradiance and ambient temperature, PV system tracks and generate around 200W. However, the conventional methods of MPPT are failed to track global maximum power point (MPP) under variable environmental conditions. From Fig 12. It is clear that the in case of conventional perturb & observe (P&O) method the oscillation around MPP is more compared to proposed Fuzzy logic controller.

Fig 12. presents the compared response of PV current, voltage and power at variable irradiance level using proposed FLC and conventional P& O method From simulation results it is clear that in case of conventional MPPT algorithm, PV current, voltage and power waveforms have oscillation around MPP compared to the proposed Fuzzy logic based MPPT algorithm. Fig 13 depicts the simulated responses using proposed and conventional MPPT methods at constant irradiance as well as varying temperature. Simulated response explain the effectiveness of MPPT & SVPWM controller

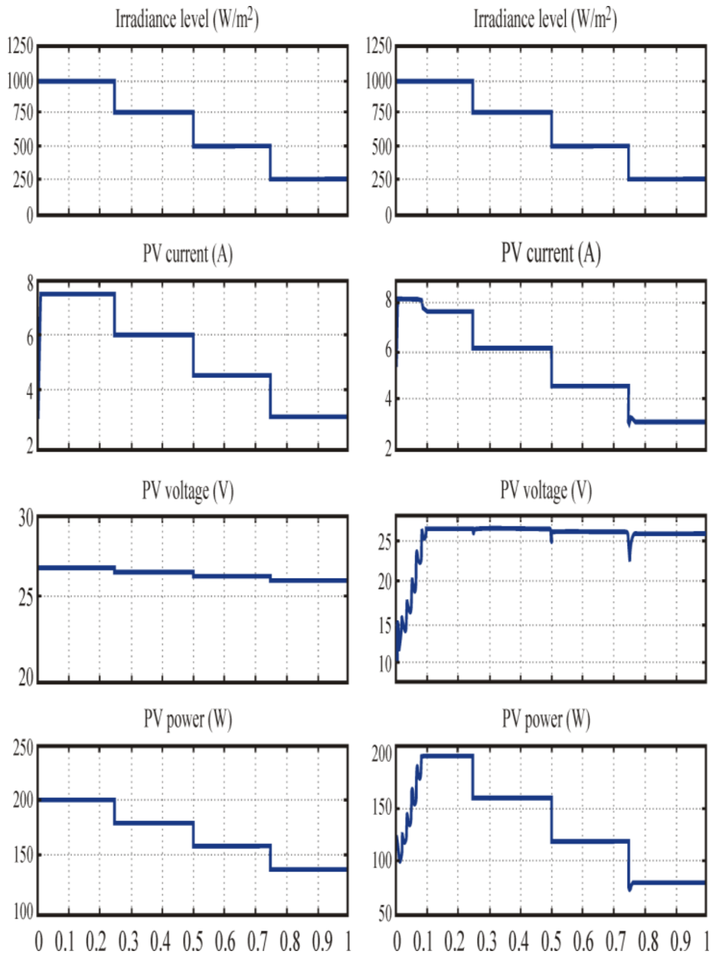

(a) With proposed control (b) With conventional P & O control

Fig. 12 Simulated responses of the proposed integrated inverter structure for grid connected PV system at variable irradiance condition (a) proposed control (b) conventional MPPT

which makes high tracked efficient system and has negligible oscillation around MPP compared to conventional MPPT control.

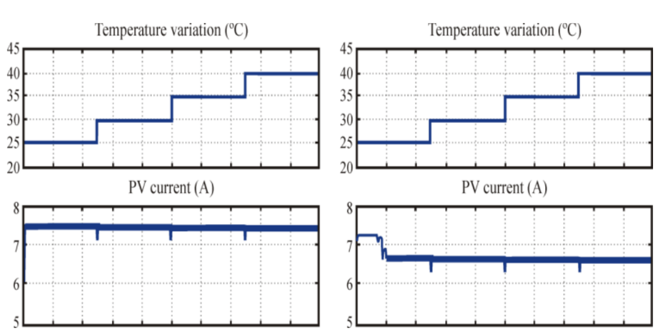

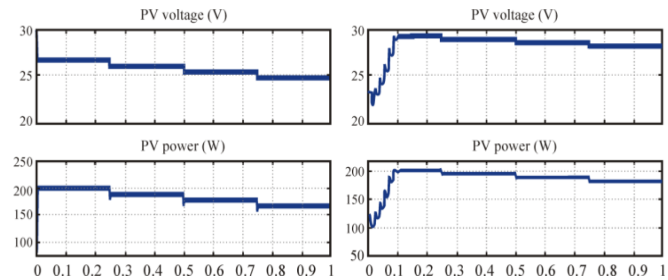

(a) With proposed control (b) With conventional control

Fig. 13 Simulated responses of the proposed integrated inverter structure for grid connected PV system at variable ambient temperature condition (a) proposed control (b) conventional control.

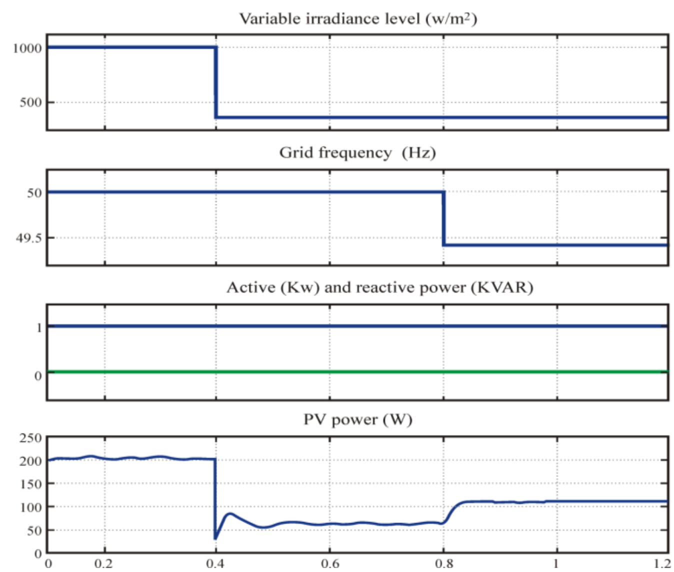

Fig. 14 Simulated responses under variation in grid frequency. Irradiance level, grid frequency, active and reactive power, frequency response of PV generator

Fig 14 depicts the simulated results of impact of grid frequency on the system performance, with sudden variation in insolation. A step change in insolation is given at t=0.4 sec and in frequency step change of -0.6 Hz is applied at t=0.8 sec. The PV array output reduces because of step change of solar insolation at t = 0.4 sec, on the other hand, because of frequency decrement after PV power increment, a frequency response is obtained. Hence in case of frequency variation, the proposed controller frequency response works effectively.

5. Experimental Results

Fig 15 shows the hardware set up developed for the verification and validation of performance of proposed controller. The simulation model implemented in Simulink is run on dSPACE DS1104. For laboratory set up, Multimeter, oscilloscope, power quality analyzer are provided for measuring parameters. Using dSPACE real-time control, the fuzzy based MPPT and SVPWM inverter control have been implemented using MATLAB/Simulink interfaced dSPACE. Zeta converter is connected to PV module for laboratory prototype.

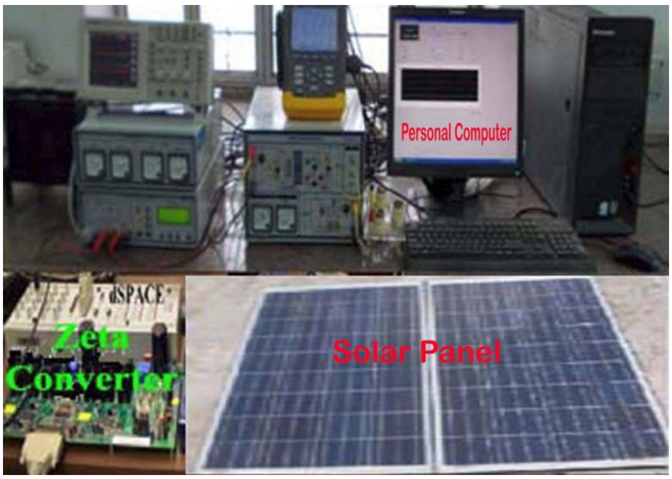

Fig. 15 Experimental setup of PV system with adaptive Fuzzy Logic MPPT

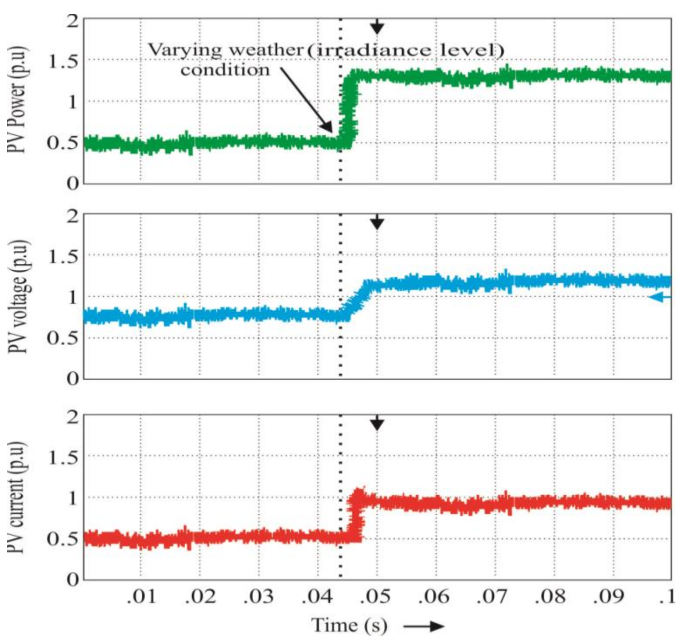

Fig. 16 Hardware responses at variable weather condition using proposed MPPT

DSP Card and dSPACE data Acquisition control has been employed for this experimental work. LTS 25-NP and voltage divider sensors are employed for the measurement of PV sourced current and voltage respectively. After measurement, these parameters are linked to dSPACE using A/D converter which is programmed in SIMULINK MPPT control block. The experimentation is performed under varying operating conditions. Fig 16 depicts the performance of the proposed controller under variable weather conditions. Practical responses reveal that the optimum power is obtained faster and MPP is obtained with negligible fluctuation compared to classical controller. The FLC and SVPWM controllers always try to bring the new operation point by forcing the power under varying transient conditions. Fig 17 shows the practical responses of PV voltage, current, grid voltage and current under standard test conditions. The experimental results justify the effectiveness of the proposed MPPT controller which performs unity power factor operation.

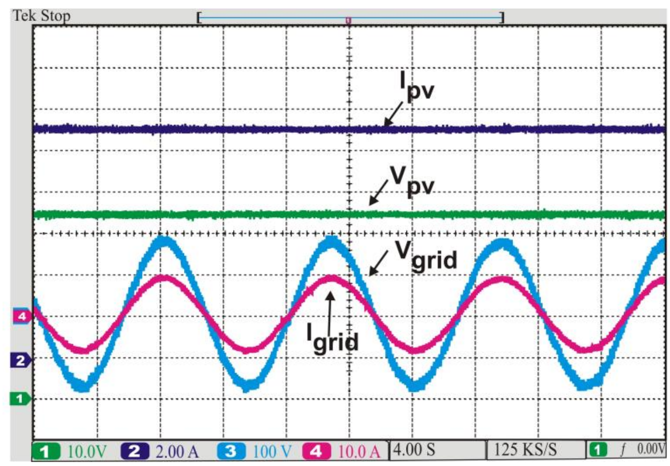

Fig. 17 Practical responses of PV voltage, current, grid voltage and current under standard test conditions.

The practically obtained inverter voltage, utility voltage and inverter current are depicted by Fig 18 reveal that the inverter voltage is completely synchronized with utility voltage.

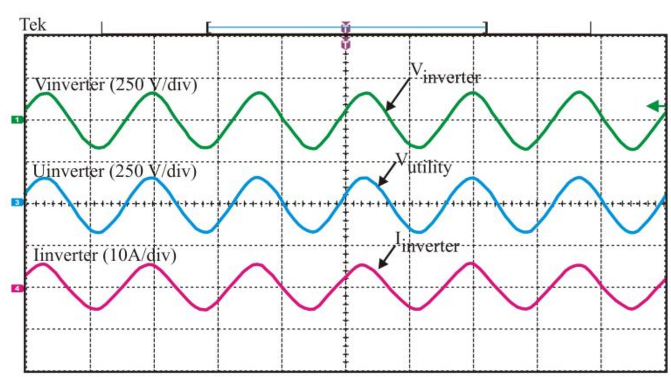

Fig. 18 Practically obtained inverter voltage, utility voltage and inverter current

The performance of the MPPT and inverter controllers has been validated under transient weather conditions. Fig 19 presents the synchronized inverter and utility voltage under transient operating conditions.

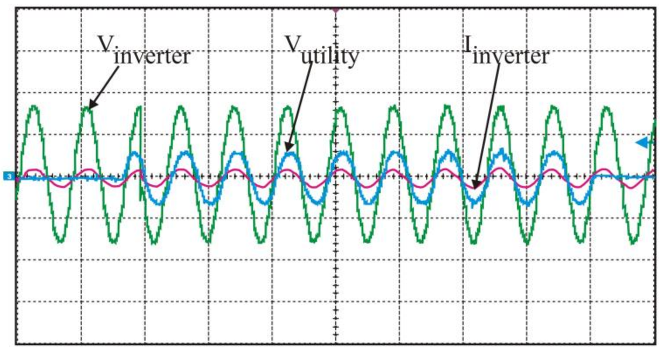

Fig. 19 Synchronized inverter and utility voltage under transient operating conditions

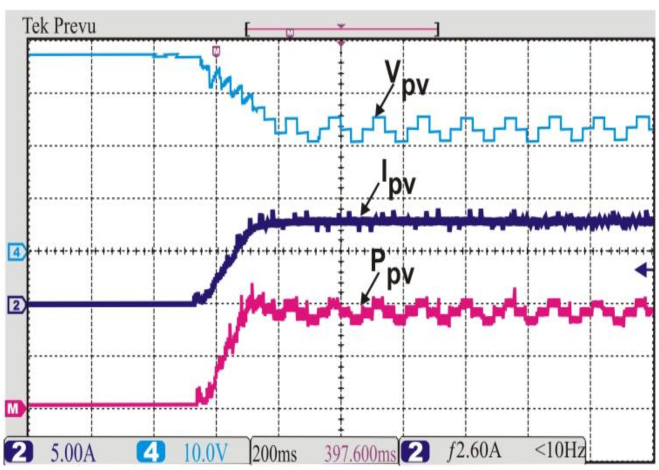

(a)

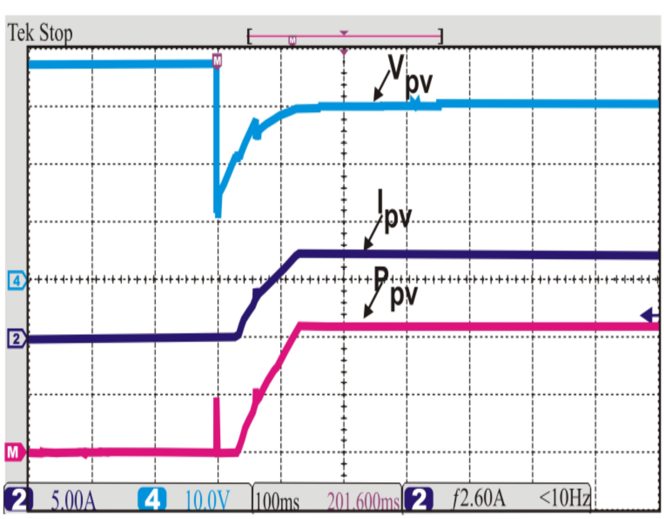

(b)

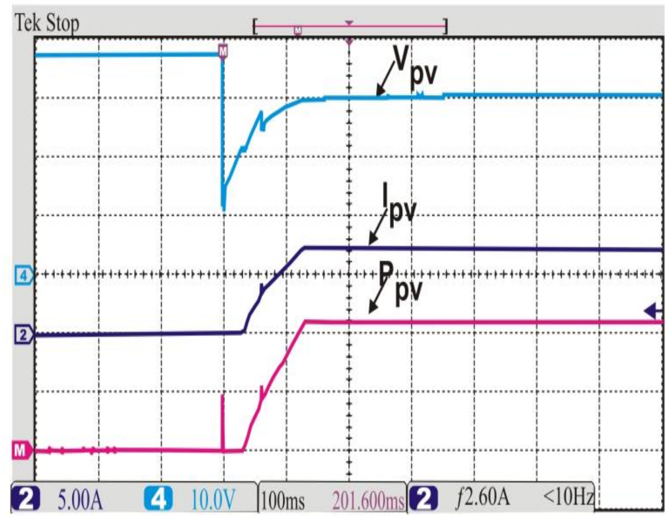

(c)

Fig. 20 Comparison waveform of PV voltage, current and power with (a) conventional P & O (b) INC MPPT(c) proposed FLC MPPT controller

Fig 20 (a), (b) and (c) depicts the comparison waveform of PV voltage, current and power with conventional P& O, incremental conductance (INC) [7] and proposed FLC controller respectively. The experimental results validate the dynamic behavior of proposed MPPT controller with high tracking efficiency and zero oscillation around mpp compared to conventional MPPT controller excellently.

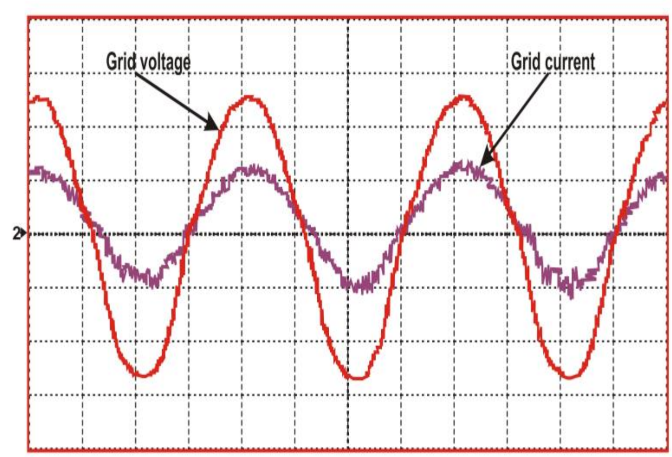

Fig. 21 Practically obtained sinusoidal grid voltage and grid current

Fig 21 shows the practical responses found at point of common coupling (PCC) which properly justify the unity power factor operation. The proposed controller makes the grid voltage and current in phase with high accuracy system design.

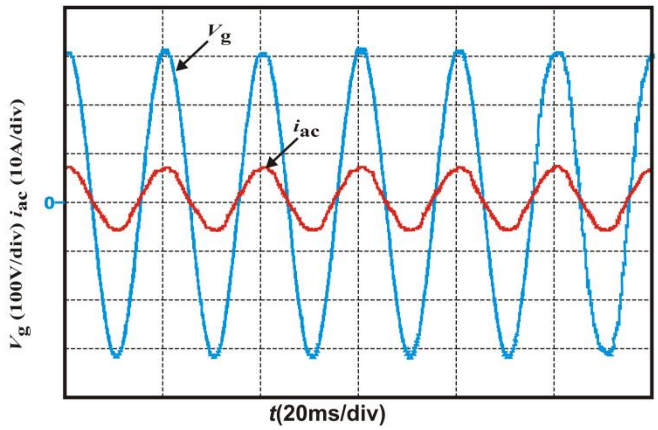

Fig. 22 Practically obtained Grid voltage and inverter current

The practical response of grid voltage and inverter current is presented by Fig 22 The inverter fed high quality sinusoidal current to the utility grid for grid synchronization which verifies the effectiveness of the proposed controller.

Table 4: Tracking and inverter efficiency of the proposed system

Irradiance level (W/m²)	Tracked PV power (W)	Maximum Tracked power(W)	Tracking efficiency (%)	Output power (W)	Inverter efficiency (%)
250	77.04	80W	96.3	66.43	86.23
500	136.64	140 W	97.6	119.01	87.1
750	157.98	160W	98.74	138.54	87.7
1100	203.19	205W	99.12	179.61	88.4
1400	219.34	220W	99.7	202.45	92.3

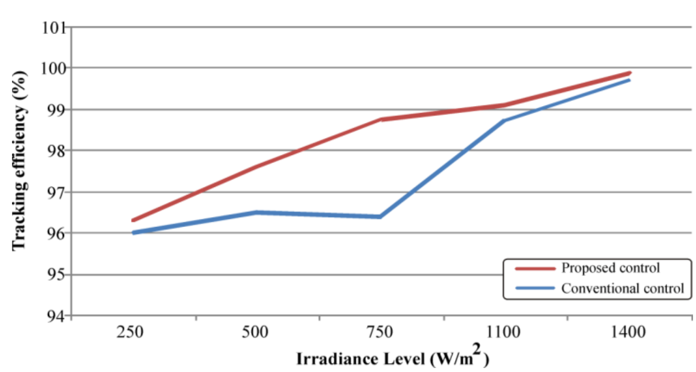

Fig. 23 Comparison of tracking power at different insolation

Fig 23 compares the tracking power at different insolation of the PV system, describing the improvement compared to the similar works in the area. Table 4 demonstrates the increase in tracking efficiency and tracked power of the 3-phase inverter integrated with utility grid under varying sun irradiance level.

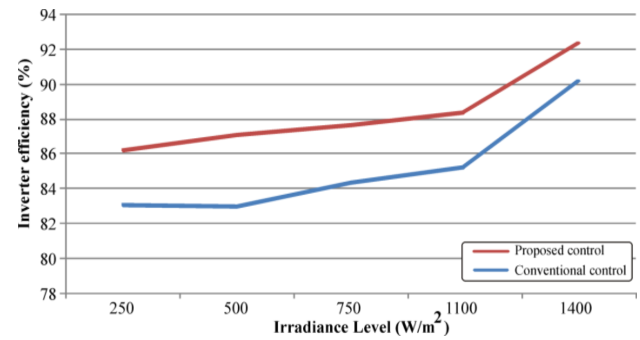

Fig. 24 Comparison of inverter efficiency at different insolation

Fig 24 compares the inverter efficiency at different insolation for proposed model with classical P&O algorithm with MPPT to the conventional control. From experimental verification it reveals that there is a considerable increment in inverter efficiency with the proposed control as compared with conventional control. The results obtained from proposed system has an average inverter efficiency about 88% for different insolation level, which is found better as compared to 83% with similar works in the area.

6. Conclusion

In this research work, the tracking and PV inverter efficiency for grid integration has been realized under different sun insolation. The FLC and SVPWM controllers for MPPT and inverter have been analyzed using dSPACE real time control board. The proposed Fuzzy MPPT controller gives rapid convergence speed and extracts maximum power from PV module. Simulated and hardware responses reveals the PV system supplies active power to the load as well as to the grid. By injecting pure sinusoidal inverter current to the utility grid the effectiveness of the proposed controller at unity power factor operation have been verified. Compared to conventional P& O and INC MPPT algorithms the proposed controllers provide better tracking and inverter efficiency.

References

[1] A. Cordeiro, D. Foito and VF. Pires, “A PV Panel Simulator Based on a Two Quadrant DC/DC Power Converter with a Sliding Mode Controller”, 4th International Conference on Renewable Energy Research and Application, pp. 928-932, 2016.

[2] S. Kirmani , M. Jamil and I. Akhtar, “Effective low cost Grid-Connected Solar Photovoltaic System to Electrify the Small Scale industry/Commercial Building”, International Journal of Renewable Energy Research, Vol.7, No.2, pp. 797-806, 2017.

[3] N. Priyadarshi, A. Anand, AK. Sharma, F. Azam, VK. Singh and RK. Sinha, “An Experimental Implementation and Testing of GA based Maximum Power Point

Tracking for PV System under Varying Ambient Conditions Using dSPACE DS 1104 Controller", International Journal Of Renewable Energy Research, Vol.7, No.1, pp. 255-265, 2017.

[4] R. Boukenoui1, R. Bradai, A. Mellit, M. Ghanes and H. Salhi, "Comparative Analysis of P&O, Modified Hill Climbing-FLC, and Adaptive P&O-FLC MPPTs for Microgrid Standalone PV System", 4th International Conference on Renewable Energy Research and Application, Italy, pp. 1095-1099. 2016.

[5] E. Kabalci, Y. Kabalci, R. Canbaz, and G. Gokkus, "Single Phase Multilevel String Inverter for Solar Applications", 4th International Conference on Renewable Energy Research and Application, pp. 109-114, 2016.

[6] N. Tutkun E. Elibol and M. Akta, "Parameter Extraction From a Typical PV Module Using a Metaheuristic Technique", 4th International Conference on Renewable Energy Research and Application, pp.755-759, 2016.

[7] S. Kahla, Y. Soufi, M. Sedraoui and M. Bechouat, "Maximum Power Point Tracking of Wind Energy Conversion System Using Multi-objective Grey Wolf Optimization of Fuzzy-Sliding Mode Controller", International Journal of Renewable Energy Research, Vol.7, No.2, pp. 926-936, 2017

[8] W. Yaïci, E. Entchev, M. Longo, M. Brenna and F. Foiadelli, "Artificial Neural Network Modelling for Performance Prediction of Solar Energy System, 4th International Conference on Renewable Energy Research And Application, pp. 1147-1151, 2016.

[9] MW. Rahman, C. Bathina, V. Karthikeyan and R. Prasanth, "Comparative analysis of developed incremental conductance (IC) and Perturb & Observe (P&O) MPPT Algorithm for Photovoltaic Applications", 10th International Conference on Intelligent System and Control (ISCO), pp. 1-6, 2016

[10] ME. Basoglu and B. Cakir, "Hardware based comparison of buckboost converter topologies in MPPT system", 9th International Conference on Electrical and Electronics Engineering (ELECO), pp. 1109-1112, 2015

[11] MA. Abolhasani, R. Rezaii, R. Beirnav and AY. Varjani, "A comparision between buck and boost topologies as module integrated converters to mitigate partial shading effect on PV arrays", 7th Power Electronics and Drive System Technologies Conference (PEDSTC), pp. 367-372, 2016

[12] M. Kaouane, A. Boukhelifa and A. Cheriti, "Implementation of incremental-counductance MPPT algorithm in a photovoltaic conversion system based on DC-DC ZETA converter", 8th International Conference on Modeling, Identification and Control (ICMIC), pp. 1195-1199, 2016

[13] H. Jinfeng and L. Shulin, "Zeta converter modeling analysis based on pulse waveform integral approach", 2016 8th International Power Electronics and Motion Control conference (IPEMC-ECCE Asia), pp. 1195-1199, 2016

[14] A. Formentini, A. Oliveri, M. Marchesoni and M. Storace, "A switched Predictive Controller for an Electrical Powertrain System with Backlash", IEEE Transactions on Power Electronics, vol. 32, no. 5, pp. 4036-4047, 2017

[15] L. Ouboubker, M. Khafallah, J Lamtekarti and A. Afia, "High Torque control performance utilizing a three level inverters with a simple switching strategy of induction machine", 2016 International Conference on Electrical and Information Technologies (ICEIT), pp. 430-435, 2016

[16] RR. Patil and SS. Hirve, "Space vector pulse width modulated inverter for grid coupled photovoltaic system at the distribution level", International Conference on Energy Efficient Technologies for Sustainability (ICEETS), pp. 560-564, 2016

[17] DC. Nabiar and CP. Jose, "A novel fuzzy based pitch angle control scheme and SVPWM based active and reactive power flow control of a permanent magnet generator based grid tied Wind Energy Conversion System", Conference on Emerging Devices and Smart Systems (ICEDSS), pp. 94-98, 2016

[18] J. Song, "Simulation of Grid-Connected Photovoltaic System", pp. 1-7.